

Reversible Hydrogels from Self-Assembling Artificial Proteins

Wendy A. Petka, James L. Harden, Kevin P. McGrath, Denis Wirtz, David A. Tirrell*

Recombinant DNA methods were used to create artificial proteins that undergo reversible gelation in response to changes in pH or temperature. The proteins consist of terminal leucine zipper domains flanking a central, flexible, water-soluble polyelectrolyte segment. Formation of coiled-coil aggregates of the terminal domains in near-neutral aqueous solutions triggers formation of a three-dimensional polymer network, with the polyelectrolyte segment retaining solvent and preventing precipitation of the chain. Dissociation of the coiled-coil aggregates through elevation of pH or temperature causes dissolution of the gel and a return to the viscous behavior that is characteristic of polymer solutions. The mild conditions under which gel formation can be controlled (near-neutral pH and near-ambient temperature) suggest that these materials have potential in bioengineering applications requiring encapsulation or controlled release of molecular and cellular species.

Thermally reversible network formation in polymeric systems is a well-known phenomenon (1–3). In aqueous solutions, synthetic polymers such as poly(vinyl alcohol) (4), proteins such as gelatin (5), and polysaccharides such as carrageenan (6) exhibit reversible gelation within prescribed limits of concentration and temperature. Despite the utility of this behavior (1), the molecular origins of gel formation in such systems are poorly understood, and opportunities for systematic engineering of gel properties are limited. Gel formation demands two seemingly contradictory kinds of behavior: Interchain interactions must be strong enough to form junction points in the molecular network, yet at the same time the chain cannot exclude solvent, or it will precipitate from solution rather than forming a swollen gel. Assignment of these two roles to different portions of a repetitive polymer such as poly(vinyl alcohol) is far from straightforward. Furthermore, the ability to tune the gel-solution (gel-sol) transition conditions is limited in such systems.

The approach to gel design presented here circumvents that problem through creation of multidomain (“triblock”) artificial proteins in which the interchain binding and solvent retention functions are engineered independently (7). The triblock architecture 3, illustrated in Fig. 1, consists of relatively short “leucine

zipper” end blocks flanking a water-soluble polyelectrolyte domain. The modular nature of the design allows independent investigation of the behavior of the individual terminal 1 and polyelectrolyte 2 blocks as well.

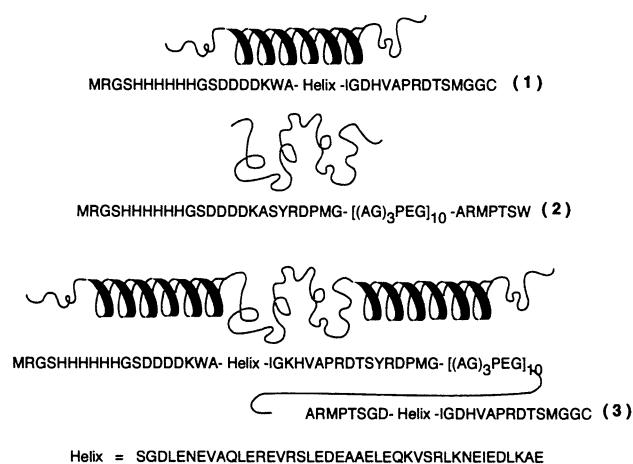
Gelation of triblock proteins such as 3 is driven by the formation of dimers (and higher order aggregates) of the terminal leucine zipper peptide domains (Fig. 2). The leucine zipper motif is characterized by a heptad periodicity generally designated abcdefg, where a and d are hydrophobic amino acids (frequently Leu, especially at position d) and the residues at positions e and g are usually charged (8). Under appropriate conditions of pH and temperature, such peptides adopt helical conformations that place the hydrophobic a and d residues on a single face of the helix. Aggregation, most often in the form of coiled-coil dimers, is then promoted by the

Fig. 1. Amino acid sequences of the three proteins studied. Protein 1 consists of 76 amino acids, 42 of which make up the leucine zipper Helix. Protein 2 consists of 122 amino acids, 90 of which make up the alanyl-glycine-rich repeat $[(AG)_3PEG]_{10}$. Protein 3 consists of 230 amino acids, 84 of which make up the Helix repeat and 90 of which make up the alanyl-glycine-rich repeat. The acidic or basic amino acids occupying the e and g positions of the Helix heptad repeat abcdefg are in bold. Single-letter abbreviations for the amino acid residues are as follows: A, Ala; C, Cys; D, Asp; E, Glu; F, Phe; G, Gly; H, His; I, Ile; K, Lys; L, Leu; M, Met; N, Asn; P, Pro; Q, Gln; R, Arg; S, Ser; T, Thr; V, Val; and W, Trp.

formation of hydrophobic interhelical interfaces, whereas the pH-dependent interactions between e and g residues modulate the stability of the coiled-coil aggregates. Aggregation number (9), dimerization specificity (10), aggregate stability (11), and aggregate structure (12) can be manipulated within wide limits through the control of chain length and amino acid sequence. The results of these studies suggest that the network junctions in gels of proteins such as 3 should be subject to similar control.

The putative leucine zipper domain (designated Helix in Fig. 1) comprises six heptad repeats. The choice of residues at positions a and d was based on the a/d residue pattern of the *Jun* oncogene product (13); and a database developed by Lupas *et al.* (14), which identifies the most probable amino acids at positions a through g in naturally occurring coiled-coil proteins, was used to select residues occupying the b, c, and f positions. Nine of the 12 e and g positions were populated by Glu residues in order to destabilize the coiled-coil structure in basic solutions and thereby to facilitate pH control of gelation and viscoelastic behavior. The polyelectrolyte domain of 3, based on the Ala-Gly-rich sequence $[(AG)_3PEG]_{10}$, was chosen because of its water solubility and absence of regular secondary structure (15)—features believed to be desirable in the design of highly swollen hydrogels (16).

Proteins 1 through 3 were prepared by bacterial expression of the corresponding artificial genes (17, 18). Circular dichroism (CD) spectroscopy confirmed the helical secondary structures of 1 and 3 at room temperature, as well as the random coil character of 2 (Fig. 3A) (19). In dilute solution, 1 and 3 exhibited thermal unfolding transitions, with the temperature of the transition midpoint (T_m) rising in each case from $\sim 30^\circ\text{C}$ at pH 11 to $\geq 80^\circ\text{C}$ at pH 6 (Fig. 3B) because of progressive neutralization of the predomi-



W. A. Petka and D. A. Tirrell, Department of Polymer Science and Engineering, University of Massachusetts, Amherst, MA 01003, USA. J. L. Harden and D. Wirtz, Department of Chemical Engineering, Johns Hopkins University, Baltimore, MD, 21218, USA. K. P. McGrath, Science and Technology Directorate, U.S. Army Natick Research Development and Engineering Center, Natick, MA 01760, USA.

*To whom correspondence should be addressed.

nantly acidic charged residues with decreasing pH (20). The abrupt increase in T_m between pH 7.5 and 6 is characteristic of coiled-coil peptides in which positions e and g are occupied predominantly by acidic residues (13). At pH values of 5 and below, no transitions were observed for either protein at temperatures below 100°C, and the helical content decreased only slightly over the temperature range from 0° to 100°C. Acidic conditions stabilize the helix sufficiently that no thermal denaturation of 1 or 3 was observed.

The gel-sol behavior of 3 in concentrated solution may be anticipated from the dilute solution behavior presented above. In a low-pH solution, the Glu side chains are protonated and the stability of the coiled-coil aggregates increases. Furthermore, protonation of the Glu residues in the polyelectrolyte linker domain causes the linker to collapse to a hydrophobic globule. Hence, precipitation of 3 should occur at low pH, and this in fact was observed. With increasing pH, progressive deprotonation of the Glu residues occurs, resulting first in swelling of the collapsed spacer block and eventually, at higher pH, in the dissociation of coiled-coil domains because of repulsive electrostatic interactions between predominantly negatively charged end blocks. Thus, in a certain range of pH, the protein should form a thermoreversible physical gel, where the reversibility of the gelled state results from thermal dissociation of the coiled-coil domains. At sufficiently high pH, a viscous solution of predominantly nonassociated proteins results. This proposed scenario is shown schematically in Fig. 2 and is borne out by simple visual observation: Aqueous solutions of 3,

which flow readily at pH 10, exhibit no visible flow on a time scale of hours upon acidification to pH 7. Aqueous solutions of either 1 or 2 do not gel at any pH, indicating that both aggregating terminal groups 1 and a spacer block 2 are necessary constituents of a gel-forming protein of this type.

In order to investigate the pH and temperature dependence of gelation, we used diffusing wave spectroscopy (21), a noninvasive optical technique based on dynamic light scattering in the multiple scattering limit, to deduce the viscoelastic behavior of 3 by monitoring the thermally induced fluctuations of a dilute suspension of added scattering particles (22). The time-averaged mean-square displacement (MSD) of the tracer particles as a function of time, $\langle r^2(t) \rangle$, may be obtained from the dynamic intensity autocorrelation function of light that is multiply scattered from these tracer particles (23). The MSD of the tracer particles contains essential information about the viscoelastic properties of the embedding medium. In particular, it can be shown that the MSD of the tracer particles is related to the shear creep compliance $J(t)$ of an incompressible embedding medium by $J(t) = (\pi a/k_B T) \langle r^2(t) \rangle$, where a is the radius of a tracer particle and $k_B T$ is the thermal energy. Equivalently, the complex shear modulus $G^*(\omega)$ may be obtained from $G^*(\omega) = k_B T / (i\omega \pi a \langle \tilde{r}^2(\omega) \rangle)$, where $\langle \tilde{r}^2(\omega) \rangle$ is the Fourier transform of $\langle r^2(t) \rangle$. In a viscous liquid, the tracer particles may freely diffuse, resulting in a MSD that increases linearly with time; whereas in an elastic medium, the amplitude of the tracer particle fluctu-

ations is limited, resulting in a plateau in the MSD (23). In a viscoelastic medium, the MSD will show some aspects of each limiting behavior. The MSDs measured for protein 3 (5% w/v in 10 mM tris buffer at 23°C) at pH 8.0, 8.8, and 9.5 are shown in Fig. 4A. At pH 8.0, the MSD exhibited a plateau that is characteristic of an elastic gel with a plateau modulus $G'_p \cong 200$ Pa near $\omega = 100$ s⁻¹. Such gel behavior was observed for protein concentrations above about 4% w/v. At pH 8.8, this plateau region was reduced to an inflection point, whereas at pH 9.5, the MSD increased with time as in a viscous liquid. These data show a progressive transformation from elastic to viscoelastic to viscous behavior and suggest that the gel point lies between pH 8.0 and 9.5.

The thermal dependence of gelation for 3 was investigated by cycling a 5% gel through a series of temperatures ranging from 23° to 55°C at pH 7.8. The MSD versus time at various temperatures is plotted in Fig. 4B. The solid curves in Fig. 4B show the data obtained during the heating portion of the cycle; the dashed curve shows the MSD after cooling from 55° back to 23°C. These data show that as the temperature was increased to 55°C, the gel progressively became a fluid. Furthermore, the gel state was recovered upon cooling back to 23°C from the fluid

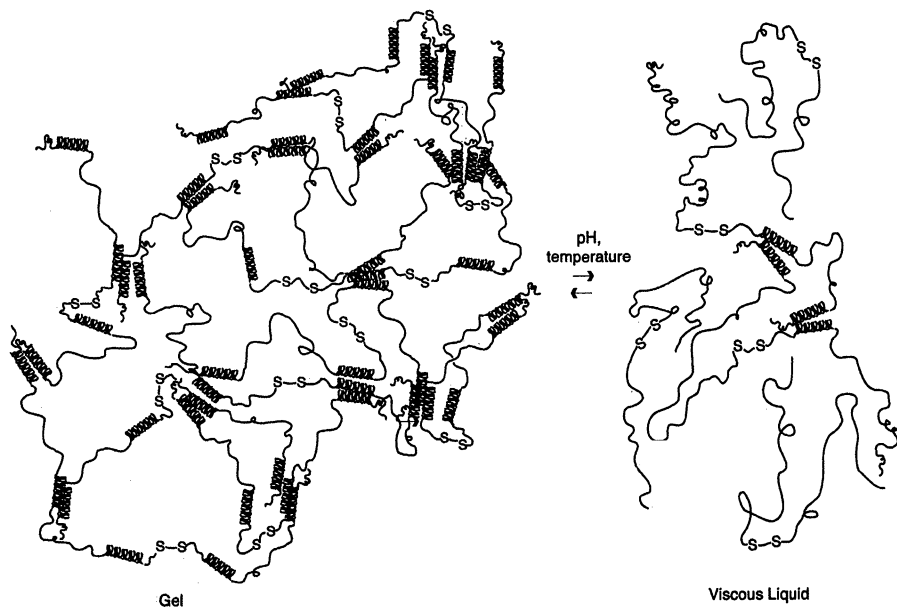


Fig. 2. Proposed physical gelation of monodisperse triblock copolymer 3. The chains are drawn as disulfide-linked dimers, joined through their COOH-terminal cysteine residues. Analysis with Ellman's reagent confirmed the absence of free thiols under the conditions used for spectroscopic and scattering studies.

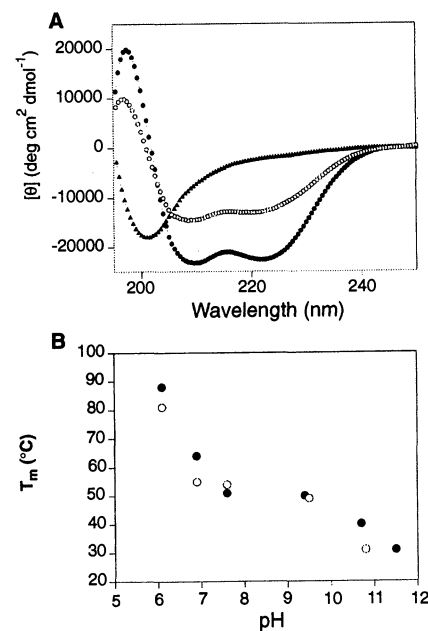


Fig. 3. (A) Secondary structural analyses of proteins 1 (●) (5 μM), 2 (▲) (5 μM), and 3 (○) (5 μM), using CD spectroscopy. Spectra were recorded at 25°C in 10 mM NaH₂PO₄ and 150 mM NaCl (pH 7.4 upon addition of 1 N NaOH). (B) Thermal denaturation T_m of proteins 1 (●) (5 μM) and 3 (○) (5 μM), monitored at 222 nm as a function of pH. Measurements were made in 10 mM NaH₂PO₄ and 150 mM NaCl (pH 7.6). T_m was determined by taking the first derivative of the CD signal $[\theta]_{222}$ with respect to temperature (K⁻¹).

state at 55°C. However, a slight hysteresis occurred after a complete cycle of heating to 55°C and returning to 23°C. This hysteresis suggests that there is a curing time associated with the refolding of the coiled-coil network junctions into the associated state. The 2- to 3-hour equilibration time allotted between 6-hour experiments was insufficient for the gel to recover its original state.

The gelation behavior of polymers such as **3** illustrates the advantages of biological synthesis and assembly processes used in combination with concepts drawn from macromolecular materials science. The triblock protein design introduced here preserves the dimerization function of the leucine zipper domain but turns that function toward entirely new objectives. Protein-protein recognition, which in nature might lead to DNA binding, now results in the formation of switchable hydrogels. The biosynthetic approach allows precise and independent control of the length, composition, and charge density of the polyelectrolyte domain and of each of the relevant architectural features of the associative end blocks. For instance, modified versions of **3** in which one acidic leucine zipper domain is replaced by a basic one undergo the gel-sol transition at much higher temperature than does unmodified **3** (24). Such control is valuable in designing hydrogels of predetermined physical and biological properties (such as strength, porosity, and sensitivity to enzymatic degradation) and

makes these triblock copolymer systems attractive candidates for use in molecular and cellular encapsulation and in controlled reagent delivery.

References and Notes

1. K. Te Nijenhuis, *Thermoreversible Networks: Viscoelastic Properties and Structure of Gels* (Springer-Verlag, Berlin, 1997).
2. A. H. Clark and S. B. Ross-Murphy, *Adv. Polym. Sci.* **83**, 57 (1987).
3. J.-M. Guenet, *Thermoreversible Gelation of Polymers and Biopolymers* (Academic Press, London, 1992).
4. G. Rehage, *Kunststoffe* **53**, 605 (1963).
5. K. Te Nijenhuis, *Colloid Polym. Sci.* **259**, 522 (1981).
6. E. R. Morris, D. A. Rees, C. Robinson, *J. Mol. Biol.* **138**, 349 (1980); H. Grasdalen and O. Smidsrod, *Macromolecules* **14**, 1845 (1981).
7. For a discussion of protein engineering of materials, see K. McGrath and D. Kaplan, Eds., *Protein-Based Materials* (Birkhauser, Boston, 1997); M. T. Krejchi et al., *Science* **265**, 1427 (1994); S. M. Yu et al., *Nature* **389**, 167 (1997).
8. W. H. Landshultz, P. F. Johnson, S. L. McKnight, *Science* **240**, 1759 (1988).
9. P. B. Harbury, T. Zhang, P. S. Kim, T. Alber, *ibid.* **262**, 1401 (1993).
10. K. J. Lumb and P. S. Kim, *ibid.* **268**, 436 (1995); E. K. O'Shea, R. Rutkowski, W. F. Stafford III, P. S. Kim, *ibid.* **245**, 646 (1989).
11. S. Y. M. Lau, A. K. Taneja, R. S. Hodges, *J. Biol. Chem.* **259**, 13253 (1984).
12. K. J. Lumb and P. S. Kim, *Biochemistry* **34**, 8642 (1995).
13. E. K. O'Shea et al., *Cell* **68**, 699 (1992).
14. A. Lupas, M. V. Dyke, J. Stock, *Science* **252**, 1162 (1991).
15. K. P. McGrath, M. J. Fournier, T. L. Mason, D. A. Tirrell, *J. Am. Chem. Soc.* **114**, 727 (1992).
16. N. A. Peppas and R. Langer, *Science* **263**, 1715 (1994); R. Yoshida et al., *Nature* **374**, 240 (1995).
17. Oligonucleotides were synthesized on a Biosearch Model 8700 DNA synthesizer [L. J. McBride and M. H. Caruthers, *Tetrahedron Lett.* **24**, 245 (1983)] and ligated into the polylinker region of cloning vector pUC18 [C. Yanisch-Perron, J. Vieira, J. Messing, *Gene* **33**, 103 (1985)]. A 213-base pair (bp) fragment encoding **1** was ligated into the Eco RI and Hind III restriction sites of pUC18 to yield pWAP-L2A; similar treatment of a 351-bp fragment encoding **2** gave pWAP-L1C. Coding and noncoding strands were verified by DNA sequence analysis. DNA fragments encoding **1** and **2** were used to assemble the artificial gene for **3**. All DNA coding sequences were isolated by Bam HI digestion and were directionally ligated into the expression vector pQE9 (Qiagen, Chatsworth, CA). The pQE9 plasmid contains a phage T5 promoter and two lac operator sequences and encodes an NH₂-terminal hexahistidine sequence that facilitates protein purification by immobilized metal affinity chromatography. Plasmids encoding **1**, **2**, and **3** were designated pQE9-L2A, pQE9-L1C, and pQE9-L2AC₁₀A, respectively. The host used for protein expression was *Escherichia coli* strain SG13009 containing repressor plasmid pREP4 (Qiagen). Cultures were grown at 37°C in 2 liters of TB medium [16 g of casein hydrolysate (Amersham), 10 g of yeast extract, and 5 g of NaCl per liter] with ampicillin (100 µg/ml) and kanamycin (50 µg/ml) until the optical densities (600 nm, OD₆₀₀) were in excess of 2. Isopropyl-β-thiogalactoside (IPTG) (1 mM) was added, and protein synthesis was induced for a period of 4 hours at 37°C. The cells were then sedimented by centrifugation (at 22100g for 30 min) and 50 ml of 6 M guanidine-HCl buffer containing Na₂HPO₄ (0.1 M, pH 8) was added. The cells were lysed at -80 °C, and the supernatant was collected for protein purification. Purification of the target proteins was achieved by metal affinity chromatography using a nickelnitrilotriacetic acid (Ni²⁺-NTA) resin supplied by Qiagen. Yields of **1**, **2**, and **3**

were 122 mg, 26 mg, and 56 mg per liter of growth medium, respectively.

18. Proteins **1**, **2**, and **3** were further purified by reversed-phase high-performance liquid chromatography (rpHPLC) before use. Chromatograms were acquired on a Waters instrument equipped with a Vydac C18 column (Supelco, Bellefonte, PA). Proteins were dissolved in distilled deionized water and filtered (filter pore size, 0.22 µm) before injection. Elution profiles were monitored at 215 nm with a linear gradient of water (0.1% trifluoroacetic acid) to acetonitrile that was run over a period of 60 min at a flow rate of 1 ml/min. Amino acid compositional analysis and matrix-assisted laser desorption mass spectrometry (MALDI-MS) were performed in the Analytical Chemistry and Peptide/DNA Synthesis Facility at Cornell University. Amino acid compositional analysis was done on a Pico-Tag Amino Acid Analysis System (Millipore, Bedford, MA). Amino acids were derivatized with phenyl isothiocyanate and analyzed by rpHPLC with a Nova Pack C18 column 4.6 mm by 300 mm (Waters, Bedford, MA). All amino acid analyses were within 5% of the theoretical values. For MALDI experiments, protein samples were mixed with 3,5-dimethoxy-4-hydroxycinnamic acid (for **1** and **2**) or α-cyano-4-hydroxycinnamic acid (for **3**) and irradiated at 337 nm. Detection was in the positive ion mode, with an accelerating voltage of 20 keV. Masses were as follows: **1**: calculated, 8549; found, 8548. **2**: calculated, 10,383; found, 10,433. **3**: calculated, 22,439; found, 22,478.
19. CD spectra were recorded on an Aviv 62DS spectropolarimeter (Lakewood, NJ) in 10 mM NaH₂PO₄ and 150 mM NaCl (pH 7.4), adjusted with 1 M NaOH. Final protein solution concentrations (after preparation at 1 mg/ml and filtering through cellulose acetate membranes with a pore size of 0.22 µm) were determined by amino acid analysis. Spectra were scanned from 250 to 195 nm at 1.0 nm bandwidth, with points taken every 0.5 nm. Experiments were performed in a rectangular cell with a 1-mm path length (Hellma Cells, Forrester Hills, NY) at 25°C. The instrument was calibrated with an aqueous solution of (1S)-(+)-(-)-10-camphorsulfonic acid; constant N₂ flushing was used.
20. Thermal melting curves were determined by monitoring the CD signal at 222 nm as a function of temperature. The signal was collected every 1°C upon an equilibration time of 1 min. Spectra were collected in 10 mM NaH₂PO₄ and 150 mM NaCl (pH adjusted with 1 M HCl or 1 M NaOH; equilibrated overnight). A thermostatically controlled cuvette holder (HP Model 89101A) was used to regulate the temperature to within ±0.2°C. A two-state mechanism was used to describe the equilibrium between folded and unfolded protein states. From this two-state model, the thermal unfolding temperature (the temperature at which the fraction unfolded is equal to fraction folded) was determined by taking the first derivative of the CD signal [θ]_{222 nm} with respect to 1/T [C. R. Cantor and P. R. Schimmel, *Biophysical Chemistry* (Freeman, New York, 1980), vol. 3, p. 1132]. T_m values were within ±2°C upon repeated scanning.
21. D. A. Weitz and D. J. Pine, in *Dynamic Light Scattering: The Method and Some Applications*, W. Brown, Ed. (Clarendon, Oxford, 1993), p. 719.
22. The dynamic intensity auto correlation function of light multiply scattered from a dilute suspension (0.5% solids diluted from stock) of tracer particles was measured with a Coherent Innova 308 Ar⁺ Laser source operating at 514 nm in the transmission geometry (23) and an ALV-5000 single-photon correlator with correlation software (ALV-GmbH, Langen, Germany). The tracer particles, 0.3-µm sulfonated polystyrene beads (SPS) (8.8% solids in solution, with a surface charge density of 1.5 µC/cm²), were obtained from Interfacial Dynamics Corporation, Portland, OR. Samples were placed into an optical glass cuvette 10 mm by 5 mm by 45 mm (NSG Precision Cell, Farmingdale, NY), and data were collected for 6 hours. The preparation of the suspensions of latex in protein solutions was accomplished as follows. Purified protein **3** (50 mg) was placed into the glass cuvette,

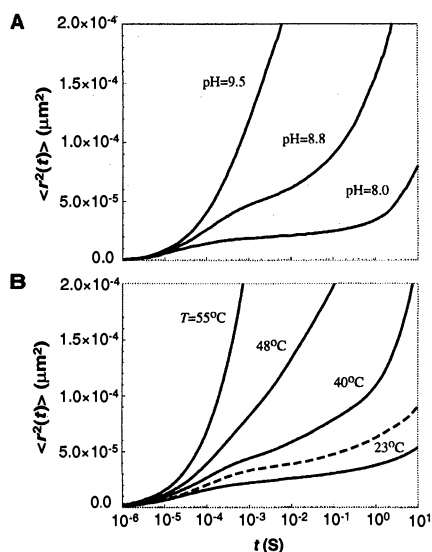


Fig. 4. (A) Log-linear plot of the MSD [$\langle r^2(t) \rangle$] as a function of time for protein **3** (5% w/v in 10 mM tris buffer at 23°C) for pH 8.0 (bottom curve), pH 8.8 (middle curve), and pH 9.5 (top curve). (B) Log-linear plot of the MSD as a function of time for protein **3** (5% w/v in 10 mM tris at pH 7.8) collected upon heating from 23°C (bottom solid curve) to 55°C (top solid curve) and upon cooling to 23°C (dashed curve).

into which 943 μl of tris(hydroxymethyl)aminomethane (tris) (buffering range of 6.9 to 7.1) and 57 μl of SPS solution were added. The sample was mixed thoroughly before 1 μl volumes of KOH (8 M) were added incrementally to change the pH. The gel containing the SPS beads was left for approximately 3 days to equilibrate, at which time additional KOH was added if the desired pH was not found. The final volume of the gel containing SPS beads was adjusted to 1 ml once the pH of the gel stabilized. The final concentration of the gel was 5% w/v. Concentration studies were made with samples prepared by diluting this volume.

23. T. G. Mason and D. A. Weitz, *Phys. Rev. Lett.* **74**, 1252 (1995); T. G. Mason, H. Gang, D. A. Weitz, *J. Mol. Struct.* **383**, 81 (1996); A. Palmer *et al.*, *Rheol. Acta* **37**, 97 (1998).
24. W. A. Petka, J. L. Harden, K. P. McGrath, D. Wirtz, D. A. Tirrell, unpublished data.
25. Supported by grants from NSF (to D.W. and D.A.T.), the Whitaker Foundation (to D.W.), and the U.S. Army Natick Research Development and Engineering Center (to D.A.T.). We thank K. Rufener and V. Viasnoff for useful discussions and assistance.

5 February 1998; accepted 3 June 1998

Atmospheric Residence Time of CH_3Br Estimated from the Junge Spatial Variability Relation

Jonah J. Colman, Donald R. Blake, F. Sherwood Rowland

The atmospheric residence time for methyl bromide (CH_3Br) has been estimated as 0.8 ± 0.1 years from its empirical spatial variability relative to C_2H_6 , C_2Cl_4 , CHCl_3 , and CH_3Cl . This evaluation of the atmospheric residence time, based on Junge's 1963 general proposal, provides an estimate for CH_3Br that is independent of source and sink estimates. Methyl bromide from combined natural and anthropogenic sources furnishes about half of the bromine that enters the stratosphere, where it plays an important role in ozone destruction. This residence time is consistent with the 0.7-year value recently calculated for CH_3Br from the combined strength estimates for its known significant sinks.

Chlorine and bromine atoms are primarily responsible for the stratospheric ozone depletion observed since the late 1970s (1). Therefore, anthropogenic production of many organochlorine and organobromine compounds has been internationally banned since January 1996 under the terms of the 1987 Montreal Protocol and its subsequent revisions. In the United States, the criterion for regulation for each compound under the Clean Air Act of 1990 is a calculated ozone depletion potential (ODP) of ≥ 0.2 , relative to CFC-11 (CCl_3F) as 1.0. Approximately half of the organobromine that reaches the stratosphere is carried there by CH_3Br for which an ODP of 0.39 has recently been estimated (2), down from 0.6 given in the 1994 Scientific Assessment of Ozone Depletion (1). A highly significant factor in ODP estimates is the atmospheric residence time (τ) for each compound, and the latest estimate for CH_3Br (2) uses a sink strength τ estimate of 0.7 years (3). However, this estimate relies on several removal sinks (gas-phase reaction with the OH radical, oceanic hydrolysis, and terrestrial reactive deposition), each with its own geographic and temporal variability. Given the uncertainties in these atmospheric processes, an estimate of τ independent of particular sources and

sinks is highly desirable. Such an independent approach was proposed by Junge in 1963 (4) based on an inverse relation between τ and the spatial variability (defined as the spatial distribution's standard deviation in mixing ratio divided by the mean mixing ratio), and elaborated theoretically since (5–8). However, the Junge relation has not previously been applied to a spatial measure of variability for determination of τ , presumably because of the lack of the necessary data on the variabilities of comparison compounds with known residence times. We have now used the empirical variabilities in the mixing ratios of ethane (C_2H_6), perchloroethylene (C_2Cl_4), chloroform (CHCl_3), and methyl chloride (CH_3Cl) in 3936 air samples collected during the NASA PEM-Tropics-A (Pacific Exploratory Mission) aircraft flights in 1996 to estimate τ for CH_3Br .

The qualitative intuition that the longer a compound lasts in the atmosphere the more likely it is to be uniformly distributed was first put into a quantitative relation in 1963 by Junge (4), who noted that "If the space and time distribution of sources and sinks were the same for all gases, the time and space variations of all constituents would be similar and the amplitudes would be proportional to τ^{-1} " (p. 2). Although these hypothetical requirements are unlikely to ever be rigorously met for any set of compounds, it is still a

useful gendanken experiment. Insufficient data on atmospheric residence times or spatial variations existed at the time to do more than state a general agreement with empirical observations. In 1974, Junge (9) compiled available data and deduced the approximate relation $\tau \times \sigma = 0.14$, in which σ is the relative standard deviation, that is, the standard deviation in the mixing ratio of a gas divided by the mean mixing ratio of that gas. He also investigated a numerical model that produced the result $\sigma = 0.0216 \times \tau^{-0.95}$. In 1983 M. Hamrud investigated the effects of different spatial arrangements of sources and sinks on the relation between τ and spatial variability in a two-dimensional numerical model (10). He found that the preexponential factor varied between 0.05 and 0.5 and the exponential term between -0.63 and -0.91 . These numerical investigations provide strong evidence that a relation between τ and spatial variability should exist in a suitable atmospheric data set, without establishing any best choice for numerical evaluation.

Various attempts have been made to derive a relation between τ and variability (mostly temporal) from first principles (5–8). With an assumed uniform sink distribution for species X, the highest mixing ratio of an individual measurement, $[\text{X}]_i$, will be set by the shortest transit time from the source (or alternatively the shortest average transit time from a number of sources). The lowest $[\text{X}]_i$ will be set by the longest transit time from the source. The mean value of all $[\text{X}]_i$ will be set by the average transit time. If two or more compounds have identical source distributions, then the range of $[\text{X}]_i$ around its mean value (for each compound) will be determined by the magnitude of the decay constant for that compound. Further, if the removal rate is proportional to the mixing ratio (as for hydroxyl-initiated oxidation), and the compound is in approximately steady state in the atmosphere, the decay constant, and therefore the variability, will be inversely proportional to τ .

In the real atmosphere, sources emit into a preexisting background of X that includes contributions from many different transit times. Junge accounted for this by estimating variability as deviations from a mean value. Additionally, some removal processes occur only at the surface (oceanic and terrestrial), while even hydroxyl-initiated oxidation is far from uniform in either space or time within the troposphere. However, Junge's result is empirical and not theoretical, and it is likely that some of these problems are averaged out in the PEM-Tropics-A data set. With several thousand air samples collected over a wide geographic area, the spatial history of the air parcels becomes essentially stochastic.

As in any investigation of the relation between τ and spatial variability, some ac-

Department of Chemistry, University of California at Irvine, Irvine, CA 92697-2025, USA.